Structural characterization of niobium-cluster anions from density-functional calculations

René Fournier,* Tao Pang, and Changfeng Chen
Department of Physics, University of Nevada, Las Vegas, Nevada 89154
(Received 19 September 1997)

We did an extensive search for the lowest-energy isomers of Nb_n^- ($n=3-8$) with a local-spin-density method. We report the calculated optimum geometries for various cluster isomers, and their vibrational frequencies and electron binding energies. We describe two simple ways to account for final-state effects on electron binding energies, based on Slater's transition state method, which yield results consistent with one another and with experiment. [S1050-2947(98)05805-3]

PACS number(s): 36.40.Mr, 31.15.Ew, 33.80.Eh, 36.40.Wa

I. INTRODUCTION

Structureless jellium models give a fair description of the size dependence of the electronic structure, thermodynamic stability, and ionization potential of groups IA and IB clusters [1,2] while providing a simple physical picture. But a detailed knowledge of the geometric structure of metal clusters may be necessary for understanding many of their properties. Structure may be responsible for certain characteristics of the optical [3] and photoelectron [4] spectra of group I metal clusters and should be even more important in the case of transition metals. The degree of symmetry, or magnitude of Jahn-Teller distortion, is probably related to cluster magnetism [5]. There are many experiments where multiple cluster isomers have been observed that sometimes have very different properties [6]. But more importantly, much physical insight is based on geometric structure. For instance, one can relate chemical reactions on clusters to those that may occur at specific surface sites having a similar structure [7], or rationalize the low reactivity or high thermodynamic stability of certain clusters from a high degree of symmetry or remarkable pattern in the atoms positions [8]. Relatively little is known about the structure of metal clusters. Many plausible structures have been obtained in theoretical studies in which the energy of many trial starting geometries is minimized and the lowest-energy minima are singled out. There are three problems with this: (1) one can fail to include important trial structures and miss the global minimum; (2) the limited accuracy of calculations can lead to incorrect energy ordering of isomers; (3) the thermodynamically most stable structure may not be the one seen experimentally, others could be favored by kinetics under some experimental conditions. Recently, a number of studies have combined experiment and theory in order to obtain structural information about metal clusters [9–13]. By comparing the observed spectra to those calculated for different possible n-atom cluster isomers, one has a more direct way to identify likely structures as those giving the best matches. It is unlikely to get a good match of spectra if the true structure is not included in the calculations, and the calculated relative energies of isomers can be used to further assess the likelihood of a structure. Gas-phase cluster spectroscopy is quite difficult because, in most experiments, clusters of different sizes coexist, they are short lived, and they are present in very low concentration. Nevertheless, a number of spectroscopic techniques developed recently can probe clusters in the gas phase: photoelectron spectroscopy (PES) of negative cluster ions [14], pulsed field ionization–zero electron kinetic energy photoelectron spectroscopy (PFI-ZEKE) [12,15], optical absorption spectroscopy by photodepletion of cluster–rare-gas van der Waals complexes [16] and infrared multiphoton decomposition (IRMPD) [17]. It is highly desirable to develop efficient computational methods that can match experiment up to fairly large cluster size in order to allow direct comparisons. Density-functional theory (DFT) is well suited for this. DFT calculations provide reasonably accurate properties for metal clusters and bulk, they can currently be done on clusters with up to about twenty metal atoms, and Slater's transition state [18,19] (STS) is a very efficient method for estimating ionization and excitation energies. We have recently used this approach to study the structure of 3- to 8-atom niobium cluster anions by comparing calculated electron binding energies (BEs) to photoelectron spectra [13]. We do not repeat the structure assignment of Nb_n^- clusters here but we give details on different methods that we used for calculating BEs. Our preferred method requires very little computing effort and is readily applicable to most DFT methods. We also report the geometric parameters and vibrational frequencies of Nb_n^- clusters and we discuss their electronic structure.

II. COMPUTATIONAL METHOD

A. Search for minimum-energy structures

We have performed calculations with the program DEMON [20] with the local-spin-density (LSD) treatment of exchange and correlation prescribed by Vosko, Wilk, and Nusair (VWN) [21]. We used a model core potential [22] to describe the $[Ar]3d^{10}4s^2$ inner shells and basis sets for the 11 valence electrons described and tested previously [23–25]. Trial geometries are optimized by minimizing the norm of the energy gradient by a standard quasi-Newton method. The resulting geometries are characterized by diagonalizing the matrix of mass-weighted energy second derivatives obtained as finite differences of analytic gradients [26]. When an optimized structure is not a minimum we distort it along the

*Present address: Department of Chemistry, York University, North York, Ontario, Canada M3J 1P3.

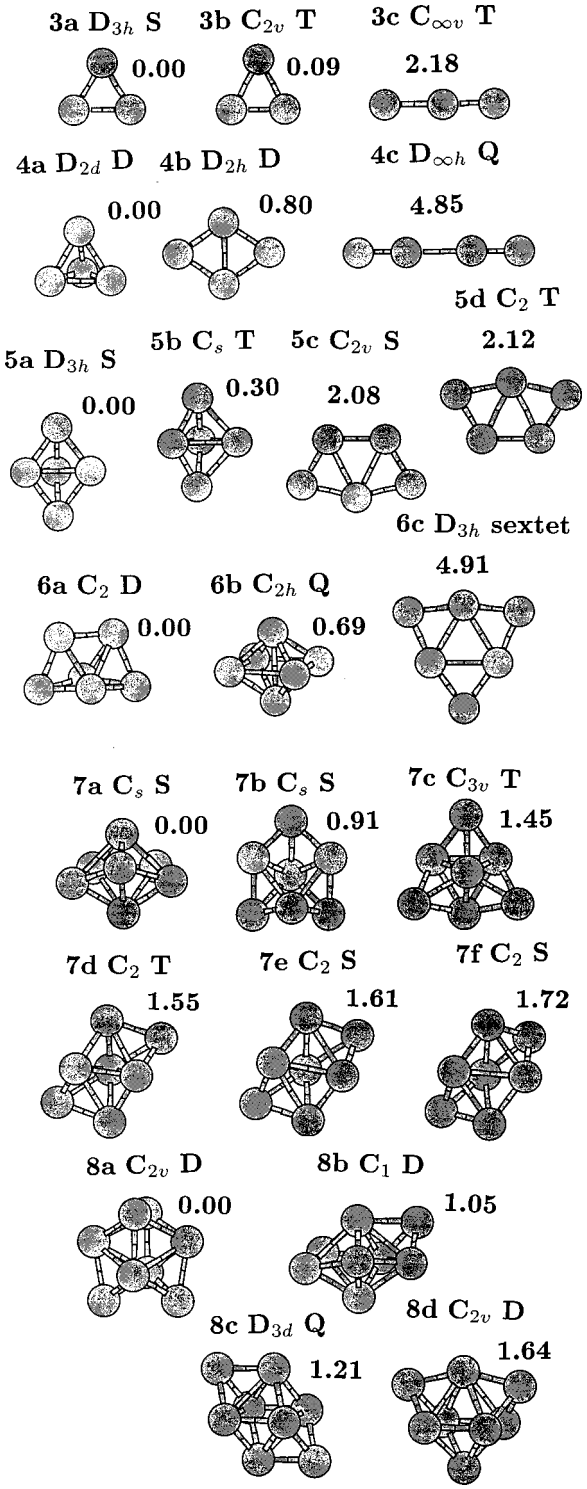

FIG. 1. Optimized Nb_n^- cluster geometries, their point-group symmetry, spin multiplicity (S=singlet, D=doublet, T=triplet, Q=quadruplet), and relative energy (eV). Bonds are drawn for atom pairs closer than 3 Å. All the structures shown are minima of the potential surface except $3c$ and $4c$ which are second-order critical points.

imaginary mode, which lowered symmetry in all cases we encountered, and resume geometry optimization. Figure 1 shows all the local minima found in this manner. The linear clusters $3c$ and $4c$, which are critical points but not minima, are also included. Apart from the structures shown in Fig. 1 and their high-symmetry counterparts (e.g., T_d for $4a$, C_{2v} for $6a$) we also considered the following starting geometries: a C_{4v} square and a planar C_{2v} end-on capped triangle Nb_4^-; a C_{4v} square-base pyramid Nb_5^-; two D_{4h} distorted octahedra (compressed and elongated forms) and a C_{5v} pentagonal pyramid Nb_6^-; four isomers of Nb_7^- obtained by adding atoms to two of the six triangular face-capping positions of $5c$ (one rearranged to $7b$, another to $7f$); and four structures for Nb_8^-, a O_h cube, a D_{4d} cube with one face rotated by 45°, a T_d tetracapped tetrahedron, and a D_{2d} structure akin to $8a$ but with only two symmetry distinct atoms. None of these trial structures led to plausible new isomers. They either have a very high energy, or possess imaginary frequencies (they are not minima), or relax to one of the structures in Fig. 1 upon optimization. We also did a few calculations (niobium atom and the clusters labeled $3a$, $5a$, and $7a$ in Fig. 1) using the gradient corrected functionals of Becke for exchange [27] and Perdew for correlation [28] (BP). With gradient corrections the results are very sensitive to the size of the grid used for numerical integration. Doubling the number of radial shells of grid points from 32 to 64 increases the BP equilibrium bond lengths by 0.02 Å to 0.15 Å but decreases the LSD-VWN bond lengths by only 0.006 Å at most. With 64 radial shells the equilibrium bond lengths obtained from BP calculations are all within 1.2% of the LSD-VWN values. We used the LSD-VWN potential and a small grid for all other clusters because the large grid BP calculations are much more time consuming, gradient corrections do not necessarily improve the predicted geometries of solids and clusters [29], and we do not have enough data to decide which method (LSD-VWN or BP) gives better results in the case of niobium clusters.

B. Electron binding energies

The lowest vertical detachment energy, or electron affinity (EA), is given rigorously in DFT by the energy difference ''D_a^{SCF}'' between the electronic ground states of the neutral and of the anion, both evaluated at the anion's equilibrium geometry. We use the subscript ''a'' to denote the highest occupied level and lowest detachment energy of the anion. The other vertical binding energies involve transitions to excited states of the neutral and cannot be obtained with the same level of rigor [30]. We estimated them using a number of methods. First, we simply take the negative of the Kohn-Sham eigenvalues of the anion:

$$D_i^{\mathrm{KS}} = -\epsilon_i .$$

Next, we can take the set of shifted Kohn-Sham (SKS) eigenvalues as approximate BEs so as to reproduce precisely D_a^{SCF}:

$$D_i^{\mathrm{SKS}} = -\epsilon_i + (D_a^{\mathrm{SCF}} + \epsilon_a).$$

The next two methods are STS approximations to the so-called ΔSCF method, which is to take the energy difference between the anion's ground state and an excited electronic configuration of the neutral. In applying the STS idea to the transition from anion to neutral, we choose the slightly more accurate generalized transition state (GTS) [19] expression:

$$D_i^{\mathrm{GTS}} = -\left[\frac{1}{4}\epsilon_i(n_i=1) + \frac{3}{4}\epsilon_i\left(n_i=\frac{1}{3}\right)\right],$$

where $\epsilon_i(n_i=\lambda)$ is the energy of orbital ϕ_i after a self-consistent-field (SCF) calculation with occupation number n_i held equal to λ. This gives very poor EAs, typically in error by 1.25 eV. But the shifted GTS BEs (D_i^{SGTS})

$$D_i^{\mathrm{SGTS}} = D_i^{\mathrm{GTS}} + (D_a^{\mathrm{SCF}} - D_a^{\mathrm{GTS}})$$

are in line with experiment [13]. Assuming that our structure assignments are correct the errors on the electron affinities are 0.00, -0.21, -0.30, -0.07, $+0.18$, and $+0.02$ eV for $Nb_3^- - Nb_8^-$, respectively. For all other BEs, the comparison to experiment is not straightforward because peaks overlap in the spectra and we cannot assign individual transitions. However, we can bring into agreement every calculated D_i^{SGTS} and observed BEs by assuming fairly systematic errors going from -0.2 to $+0.4$ eV [13]. This is the kind of accuracy that we expect for STS calculations of excitation or ionization energies in the 1–4-eV range.

Alternatively, we can view electron detachment from ϕ_i as detachment from ϕ_a followed by excitation from ϕ_i into ϕ_a in the *neutral* cluster at the *anion* equilibrium geometry:

$$D_i^{\mathrm{IE}} = D_a^{\mathrm{SCF}} + \Delta E_{ia}^{\mathrm{STS}},$$

where $\Delta E_{ia}^{\mathrm{STS}}$ is the STS excitation energy:

$$\Delta E_{ia}^{\mathrm{STS}} = \epsilon_a(n_i=n_a=\tfrac{1}{2}) - \epsilon_i(n_i=n_a=\tfrac{1}{2}).$$

With this method there is no need for a shift since D_a^{IE} is automatically equal to D_a^{SCF}. For singlet-to-singlet excitations originating from a closed-shell configuration, we can easily apply the spin multiplet (SM) method of Ziegler *et al.* [31] and get the energy of excited states that properly combine two Kohn-Sham determinants to yield a $(\alpha\beta-\beta\alpha)$ spin function. With only two unpaired electrons in the upper state, the energy can be derived from a sum rule and is

$$\Delta E_{ia}^{\mathrm{STS\text{-}SM}} = 2[\epsilon_a(n_i^\alpha=n_a^\beta=\tfrac{1}{2}) - \epsilon_i(n_i^\alpha=n_a^\beta=\tfrac{1}{2})] - [\epsilon_a(n_i^\alpha=n_a^\alpha=\tfrac{1}{2}) - \epsilon_i(n_i^\alpha=n_a^\alpha=\tfrac{1}{2})].$$

Using that expression gives another set of BEs, $D_i^{\mathrm{IE\text{-}SM}}$. Theoretically, $D_i^{\mathrm{IE\text{-}SM}}$ is our best estimate: (i) it includes the effect of orbital relaxation upon ionization precisely for the EA, which correctly reduces to D_a^{SCF}; (ii) it describes the relaxation for the other D_i's via STS for excited neutral configurations, and this is apparently more reliable than STS calculations for negatively charged clusters; (iii) it gives a balanced description of the neutral singlet and triplet states by using the spin functions $(\alpha\alpha)$ and $(\alpha\beta-\beta\alpha)$ [instead of $(\alpha\beta)$].

Before doing a transition state calculation we need the Kohn-Sham orbitals ϕ_k^0 of the ground state. Then, we converge the SCF process to a transition state by setting the occupation numbers at each SCF iteration ''n'' as follows. We calculate the overlap S_{ji} (S_{ja}) of all current orbitals ϕ_j^n with the orbital(s) ϕ_i^0 (and also ϕ_a^0 in the case of an excitation) for which we want fractional occupation. We identify the orbital (or the two orbitals) among ϕ_j^n with the largest absolute value of S_{ji} (and S_{ja} if needed) and set occupation numbers accordingly.

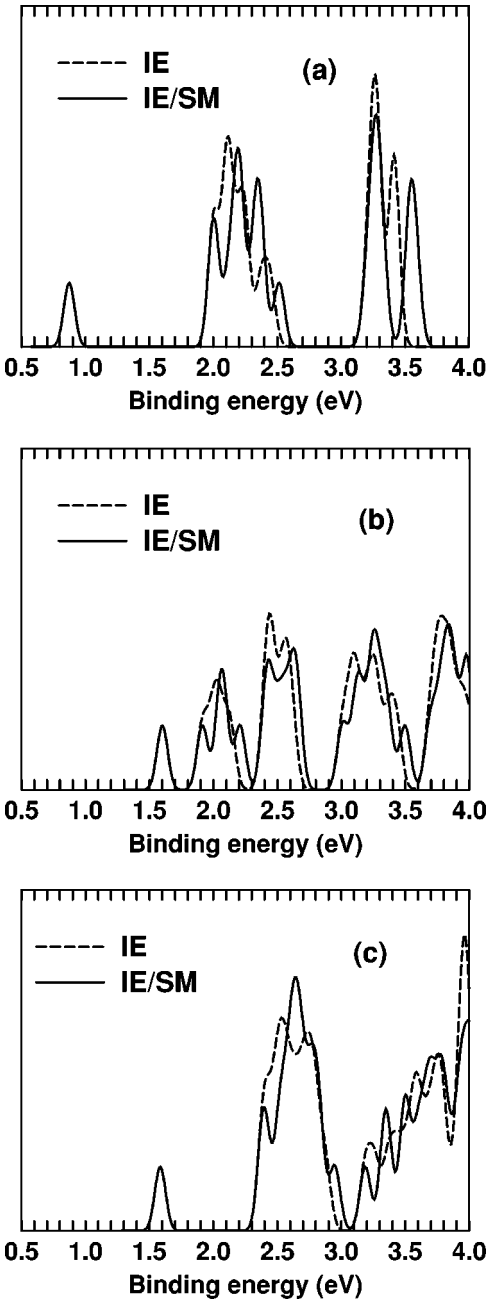

FIG. 2. Binding energies calculated with the IE-SM (full line) and IE (dashed line) methods for the lowest-energy isomers (a) $4a$, (b) $6a$, and (c) $8a$.

We will now compare the four sets of calculated BEs, which are, in order of increasing computing requirement and accuracy, D_i^{SKS}, D_i^{SGTS}, D_i^{IE}, and $D_i^{\mathrm{IE\text{-}SM}}$. Figure 2 shows D_i^{IE} and $D_i^{\mathrm{IE\text{-}SM}}$ for clusters $4a$, $6a$, and $8a$. Each discrete level was replaced by a Gaussian function with 0.1 eV width. It should be noted that the neutral ground state of $6a$ at the *anion's equilibrium geometry* is singlet: at the neutral's equilibrium geometry, we find a triplet in agreement with Goodwin and Salahub [23]. The low-energy sides of every peak in Fig. 2 coincide because they correspond to triplet states that are treated in the same way. The singlet energies are larger in

the IE-SM method by roughly 0.1 eV: the peaks extend to higher energies and there is more apparent structure with our chosen 0.1-eV Gaussian width. But overall, D_i^{IE} and $D_i^{\mathrm{IE\text{-}SM}}$ are quite similar. Because of this and of the complexity of the SM method for open-shell ground states [31], we did not compute $D_i^{\mathrm{IE\text{-}SM}}$ for other clusters.

We now compare the other two methods against the set D_i^{IE} for the clusters $3a, 4a, \ldots, 8a$, which provide a total of 132 calculated BEs. First of all, we note that the six D_a^{KS} are seriously in error: the average shift required to bring D_a^{KS} equal to D_a^{SCF} is 1.73 eV. Moreover, the shifts needed for the different clusters are far from uniform; they vary between 1.58 and 2.17 eV. Even with individual shifts for each cluster, the shifted Kohn-Sham eigenvalues D_i^{SKS} are still in error by 0.21 eV on average. This is clear in Fig. 3 where the dotted curve departs from the other two. Orbital relaxation (or ''final state effects'') is quite important [32]: it changes not only the absolute but also the relative values of the BEs.

The errors on the unshifted D_a^{GTS} are 1.27 eV on average, with a standard deviation of 0.13 eV. Such large and systematic errors are surprising considering the success of STS in calculations of the ionization potentials of small neutral molecules [33]. After shifting to reproduce D_a^{SCF}, the average absolute difference between the D_i^{SGTS} and D_i^{IE}, for 126 cases *excluding* the six D_a's (which agree by definition), is only 0.011 eV (see Fig. 3). This close agreement is reassuring and convenient. In a few cases we failed to reach convergence in SGTS calculations. When that happened, we performed an IE calculation and used D_i^{IE} in place of D_i^{SGTS}. Mixing results from the SGTS and IE methods is inconsequential because other errors, rooted in LSD theory or due to numerics or approximations, are much larger than 0.01 eV. The SGTS calculations are generally easier and constitute our method of choice.

III. RESULTS

A. Equilibrium geometries and vibrations

Comparison of our BEs to experimental spectra identifies the clusters seen experimentally as $3b$, $4a$, $5b$, $6a$, $7a$, and $8a$. This coincides with the lowest-energy isomers that we found except for $3b$ and $5b$, which are only 0.09 and 0.30 eV higher than $3a$ and $5a$, respectively. Considering all the structures of Fig. 1, and others we tried, the Nb_n^- clusters can be briefly characterized as being three dimensional, fairly compact, and having low symmetry. This contrasts with clusters of simple metals, which apparently tend to adopt more open, often two-dimensional, structures [10,11,34]. It also contrasts with structures predicted from classical potentials or effective medium theories, which typically have high symmetry. For instance, the structures predicted by the corrected effective medium (CEM) method for nickel clusters [35] closely resemble our Nb_n^- clusters except that they *all* have higher symmetry: D_{3h}, T_d, D_{3h}, O_h (which is topologically different from $6a$ but similar to $6b$), D_{5h}, and D_{2d}, for Ni_3 to Ni_8 respectively. Other LSD studies besides our own indicate that Jahn-Teller distortion is probably common among metal clusters [36].

The Nb_n^- equilibrium geometries are very similar to those calculated by the same method for the neutrals [23].

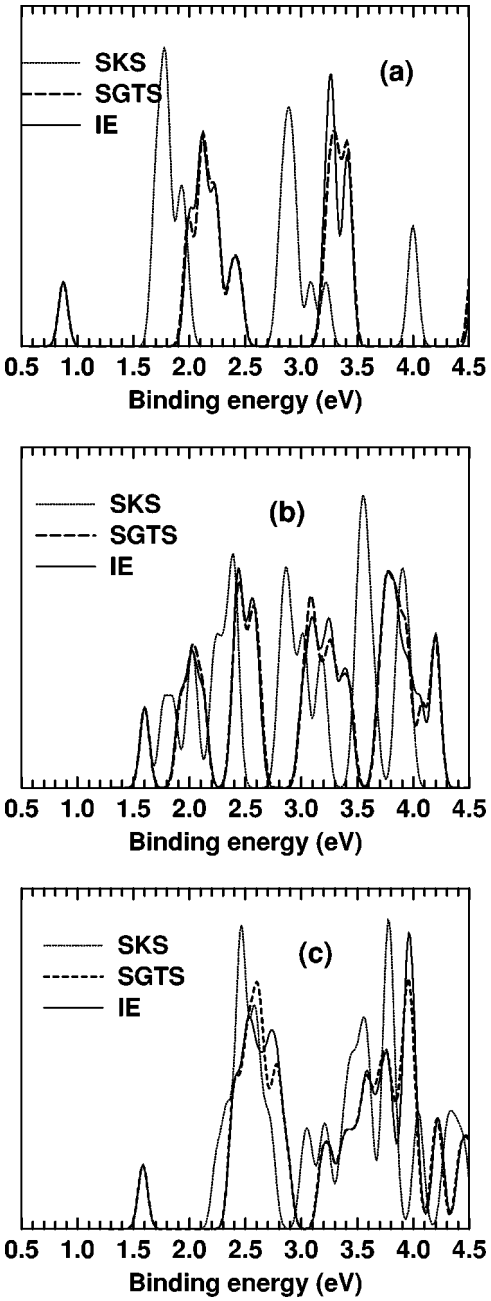

FIG. 3. The electron binding energies calculated with different methods — IE (full line), SGTS (dashed line), and SKS (dotted line) — for clusters (a) $4a$, (b) $6a$, and (c) $8a$.

The shapes are the same, but small distortions lower the symmetry in $4a$ and $6a$. The bond lengths (listed in Table I) are typically within 0.05 Å of those of the neutrals. A simple explanation for this is that, with a $4d^4 5s^1$ valence configuration, the frontier orbitals of Nb_n are essentially nonbonding, d_δ-like, orbitals. This is certainly true for Nb_2, which has the ground-state configuration $1\pi_u^4 1\sigma_g^2 2\sigma_g^2 1\delta_g^2$ [24], but it also holds approximately for larger clusters with complicated shapes. Adding or removing electrons from these nonbonding orbitals should have little effect on the bonding so it is not too surprising that the anion niobium clusters have geometries close to those of the neutrals. Likewise, one expects that the vibrational modes of the anions and the neutrals are similar. Figure 4 shows that this is indeed the case

TABLE I. Calculated LSD bond lengths and angles of the Nb_n^- clusters of Fig. 1. Numbers in parentheses indicate the number of equivalent bonds when there is more than one.

Cluster	Bond(s)	Bond lengths (Å)
$3a\ D_{3h}$		2.31 (3)
$3b\ C_{2v}$		2.21; 2.42 (2)
$3c\ C_{\infty v}$		2.11; 2.41
$4a\ D_{2d}$		2.43 (2); 2.50 (4)
$4b\ D_{2h}$		2.33 (4); 2.62
$4c\ D_{\infty h}$		2.03 (2); 2.70
$5a\ D_{3h}$		2.44 (6); 2.71 (3)
$5b\ C_s$	equatorial:	2.45; 2.77; 2.83
	axial-eq.	2.39 (2); 2.47 (2); 2.54 (2)
$5c\ C_{2v}$	perimeter:	2.42; 2.24; 2.35; 2.35; 2.24
	inner:	2.77 (2)
$5d\ C_2$	perimeter:	2.45; 2.22; 2.38; 2.38; 2.22
	inner:	2.71 (2)
	dihedral:	12°
$6a\ C_2$	rhombus:	2.42 (2); 2.51 (2); 2.81
	R_{13}, $R_{13'}$	2.61 (2); 2.89 (2)
	R_{23}, $R_{33'}$	2.41 (2); 2.38
	dihedral $211'2'$:	10°; 36°; 36°; 22°; 0°
$6b\ D_{2h}$	equatorial:	2.73 (2); 2.92 (2)
		2.49 (8); 2.98
$6d\ D_{3h}$		2.34 (6); 2.79 (3)
$7a\ C_s$	equatorial:	2.53; 2.51; 2.48; 2.48; 2.51
	axial-eq. 1:	2.49; 2.49; 2.84; 2.48; 2.84
	axial-eq. 2:	2.76; 2.76; 2.42; 2.77; 2.42
	eq. dihedrals:	22°; 36°; 36°; 22°; 0°
$7b\ C_s$	R_{12}, R_{14}	2.45 (2); 2.64 (2)
	R_{23}, R_{24}	2.47 (2); 2.58 (2)
	R_{34}, R_{35}, R_{45}	2.80 (2); 2.52; 2.36 (2)
$7c\ C_{3v}$	R_{12}, R_{13}	2.58 (3); 2.51 (3)
	R_{23}, $R_{22'}$	2.51 (6); 2.55 (3)
$7d\ C_2$	equatorial:	2.46; 2.92 (2)
	axial-eq.:	2.52 (2); 2.55 (2); 2.83 (2)
	R_{34}, R_{24}, R_{14}:	2.34 (2); 2.45 (2); 2.64 (2)
$7e\ C_2$	equatorial:	2.81 (2); 2.85
	axial-eq.:	2.42 (2); 2.64 (2); 2.87 (2)
	R_{34}, R_{24}, R_{14}:	2.32 (2); 2.36 (2); 2.62 (2)
$7f\ C_2$	equatorial:	2.84; 2.86 (2)
	axial-eq.:	2.40 (2); 2.60 (2); 2.94
	R_{34}, R_{24}, R_{14}:	2.38 (2); 2.41 (2); 2.49 (2)
$8a\ C_{2v}$	R_{12}, R_{13}, R_{14}	2.47 (4); 2.83 (4); 2.46 (2)
	R_{23}, R_{34}, $R_{44'}$	2.44 (2); 2.56 (4); 2.57
$8b\ C_1$	equatorial:	2.99; 2.52; 2.60; 2.35; 2.42
	axial-eq. 1:	2.81; 2.79; 2.54; 2.88; 2.60
	axial-eq. 2:	2.71; 2.61; 2.55; 2.47; 2.86
	axial-cap:	2.58
	eq.-cap:	2.37; 2.32
	eq. dihedrals:	12°; 25°; 28°; 19°; 3°
$8c\ D_{3d}$	$R_{11'}$, R_{12}, R_{13}	2.85 (6); 2.43 (6); 2.52 (6)
$8d\ C_{2v}$	equatorial:	2.52 (2); 2.89 (2)
	R_{12}, R_{24}	2.86 (4); 2.57 (4)
	R_{13}, R_{23}	2.39 (2); 2.41 (4)

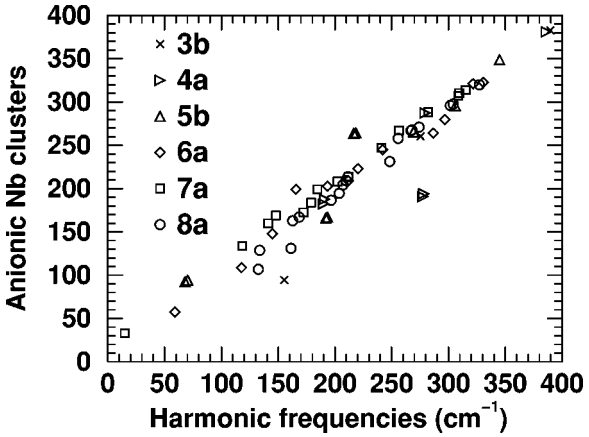

FIG. 4. Normal mode (harmonic) LSD frequencies of the niobium cluster anion isomers $3b$, $4a$, $5b$, $6a$, $7a$, and $8a$, compared to those of the corresponding neutral clusters.

for our LSD harmonic frequencies. There are only three modes (one each for $3b$, $4a$, and $5b$) for which the neutral and anion frequencies differ by more than 40 cm^{-1}. The insensitivity of equilibrium geometries and frequencies on the charge state of niobium clusters may be responsible for the relatively clean photodetachment spectra [13] and suggests that the PFI-ZEKE spectra of Nb_n could also be fairly simple.

The harmonic vibrational frequencies of all minima are reported in Table II. Frequencies typically range from 100 to 350 cm^{-1}, and the average goes from 246 cm^{-1} for Nb_3^- to an essentially converged value of 215 cm^{-1} (215, 214, and 218 cm^{-1} for the 6-, 7-, and 8-atom clusters, respectively). Judging only from the lowest frequencies there does not seem to be a simple correlation between the stability of a cluster isomer and its rigidity. The very low frequency modes in $6a$ and $7a$, 58 cm^{-1} and 33 cm^{-1} respectively, suggest that these clusters might even be fluxional at room temperature. This would be remarkable considering that niobium has one of the highest melting points (2750 K) of all elements. However, in both cases, those low frequency modes are essentially twisting motions of two atoms, the two topmost atoms of $6a$ and two of the equatorial atoms of $7a$, with very small amplitudes on all other atoms. Anharmonic force fields or molecular dynamics simulations would be required to characterize more precisely the configuration of these clusters at room temperature.

B. Electronic structure

The s, p, and d electronic densities of states (DOS) for $3b$, $4a$, $5b$, $6a$, $7a$, and $8a$ are displayed in Fig. 5. They can be described qualitatively by analogy with the orbitals of the niobium dimer [24]. Starting with the low-energy side of the DOS, there is first a strongly bonding d_π-like state, then some s-d_σ-like hybridized states that extend up to E_F, and next a large DOS associated with bonding d states extending between 0 and 3 eV below E_F. The empty states are first the antibonding s-type states just above E_F, which become hybridized with d_σ-like states at higher energies, and then antibonding d states going from about $+1$ to $+4$ eV, which are, in order of increasing energy, of d_δ, d_π, and d_σ character. In the simplest picture, the valence states of n-atom

TABLE II. Harmonic vibrational frequencies (cm^{-1}).

$3a$:	264, 264, 387
$3b$:	94, 260, 383
$4a$:	182, 188, 191, 194, 287, 381
$4b$:	131, 140, 244, 294, 314, 344
$5a$:	93, 94, 166, 167, 264, 264, 265, 295, 349
$5b$:	102, 139, 155, 169, 205, 225, 243, 310, 350
$5c$:	26, 85, 163, 188, 202, 215, 265, 340, 350
$5d$:	63, 92, 161, 170, 180, 227, 239, 330, 353
$6a$:	58, 109, 148, 199, 203, 209, 223, 245, 264, 279, 321, 323
$6b$:	46, 83, 133, 142, 165, 168, 183, 235, 248, 256, 258, 329
$6c$:	38, 77, 78, 103, 126, 144, 170, 181, 254, 261, 274
$7a$:	33, 134, 160, 169, 172, 184, 199, 208, 214, 247, 267, 288, 307, 310, 314
$7b$:	99, 104, 129, 148, 157, 170, 182, 210, 214, 248, 258, 277, 286, 306, 324
$7c$:	74, 92, 103, 140, 173, 174, 179, 195, 220, 231, 242, 265, 289, 299, 308
$7d$:	67, 95, 111, 136, 152, 172, 213, 215, 219, 235, 249, 257, 289, 320, 335
$7e$:	35, 86, 115, 130, 157, 177, 197, 214, 224, 228, 253, 266, 299, 338, 340
$7f$:	56, 92, 131, 156, 158, 172, 182, 205, 232, 239, 242, 269, 285, 318, 338
$8a$:	107, 129, 131, 163, 167, 186, 195, 204, 209, 214, 231, 258, 267, 268, 270, 296, 298, 320
$8b$:	78, 104, 126, 138, 153, 169, 172, 197, 204, 213, 222, 227, 258, 263, 285, 297, 312, 323
$8c$:	110, 111, 112, 151, 151, 200, 200, 210, 210, 219, 224, 224, 238, 238, 286, 289, 305, 307
$8d$:	76, 124, 138, 139, 146, 169, 175, 183, 202, 216, 228, 238, 243, 245, 253, 289, 319, 325

niobium clusters consist of $6n$ orbitals formed by combining the five d and single s orbitals of each of the n atoms, with very small p contributions as seen in Fig. 5. For each cluster, we have used the $6n$ lowest-energy valence eigenvalues to calculate the mean, rms deviation, and a width taken simply as the difference between the highest and lowest eigenvalues. As the cluster size increases the mean of the eigenvalues goes down and correlates roughly with the increase of the electron affinity of a conducting sphere [2]. The mean also shows interesting variations with geometric structure: with few and minor exceptions, it is highest for the most stable and most compact isomers and is lowest for the more open and least stable structures. The rms deviation increases steadily with cluster size, from 1.58 to 2.08 eV, as the DOS evolves from a few discrete levels toward bulklike energy bands. We expected that the rms deviation might be larger for the most stable cluster isomers because the separation of bonding and antibonding levels is presumably larger in strongly bound clusters, but such is not the case. The rms deviation changes very little from one cluster isomer to another and is not correlated with stability. The width also increases steadily with cluster size and shows more pronounced but apparently nonsystematic variations with geometric structure. The local (atom projected) DOS for the most stable clusters shows that different atoms in a cluster are similar. However, the chemically important frontier orbitals are rather strongly localized in $5b$, $6a$, and $7a$: in these clusters, but not in $8a$ or the smaller clusters, the highest occupied molecular orbital (HOMO) has small amplitudes on atoms where the lowest unoccupied molecular orbital (LUMO) has large amplitudes, and vice-versa.

Some of the cluster anions have a positive energy HOMO. In those cases, by virtue of Janak's theorem [37], some fractionally charged states would have a lower energy: varying the number of electrons, the lowest energy would be achieved with a charge such that ϵ^{HOMO} is zero. Likewise, the exact LSD solution for singly charged anions having positive ϵ^{HOMO} must have a fraction of an electron delocalized in free space. This unphysical situation is due to the spurious self-interaction in LSD, which leads to an incorrect $(+1/r)$ long-range behavior of the effective one-electron potential. As clusters get bigger, the self-interaction becomes less and the anions should become stable in LSD. Using the ϵ^{HOMO} of the anions and neutrals, and assuming that ϵ^{HOMO} varies linearly with number of electrons, we can estimate the maximum negative charge for which a stable exact LSD solution exists. Taking only the most stable isomers, and going in order from the dimer to the 6-atom cluster, these maximum negative charges are -0.77, -0.78, -0.95, -0.97, and -0.99; the anions of the 7- and 8-atom clusters are stable in LSD. These numbers suggest that the problem is not serious except maybe for the dimer, trimer, and the T_d isomer of Nb_4 for which the maximum negative charge is -0.84. Shore *et al.* [38], who studied this problem for H^-, suggested that good results can be obtained even for atoms if the electrons are constrained to stay near the nucleus with a spherical potential barrier at a large radius. By using a standard localized basis set we achieve essentially the same thing: the incorrect LSD potential should drive a fraction of an electron away from the smaller cluster anions, but our approximate LSD solution does not permit this unphysical behavior. We believe that anion instability in DFT becomes problematic only for very small molecules or clusters, and only when highly accurate solutions, expressed in a large basis set, are sought [39].

C. Size evolution of properties

Table III shows the binding energy per atom, $Nb_n^- \rightarrow (n-1)Nb + Nb^- + nB$ eV, and the energy required for dissociation, $Nb_n^- \rightarrow Nb_{n-1}^- + Nb + E$ eV, disproportionation, $2Nb_n^- \rightarrow Nb_{n-1}^- + Nb_{n+1}^- + D$ eV, and ionization $Nb_n^- \rightarrow Nb_n + e^- + A$ eV. Judging from values of E and D in Table III, the four- and seven-atom Nb anion clusters ($4a$ and $7a$) are relatively more stable than the rest. Four- and seven-atom *neutral* and *cationic* niobium clusters also show particular stability according to collision-induced dissociation experiments [40] and to DFT calculations [23]. Stability in Nb clusters is determined more by the number of atoms and atomic structure, which affects the relative orientation of orbitals and number of dangling bonds, than by the number of valence electrons and electronic shell closing effects. We note that the ionization potentials of Nb clusters [40,41] show no evidence of shell closing effects whereas those of Cu clusters [42] do follow a pattern typical of jellium models. Overall, the binding energy per atom (B) increases with

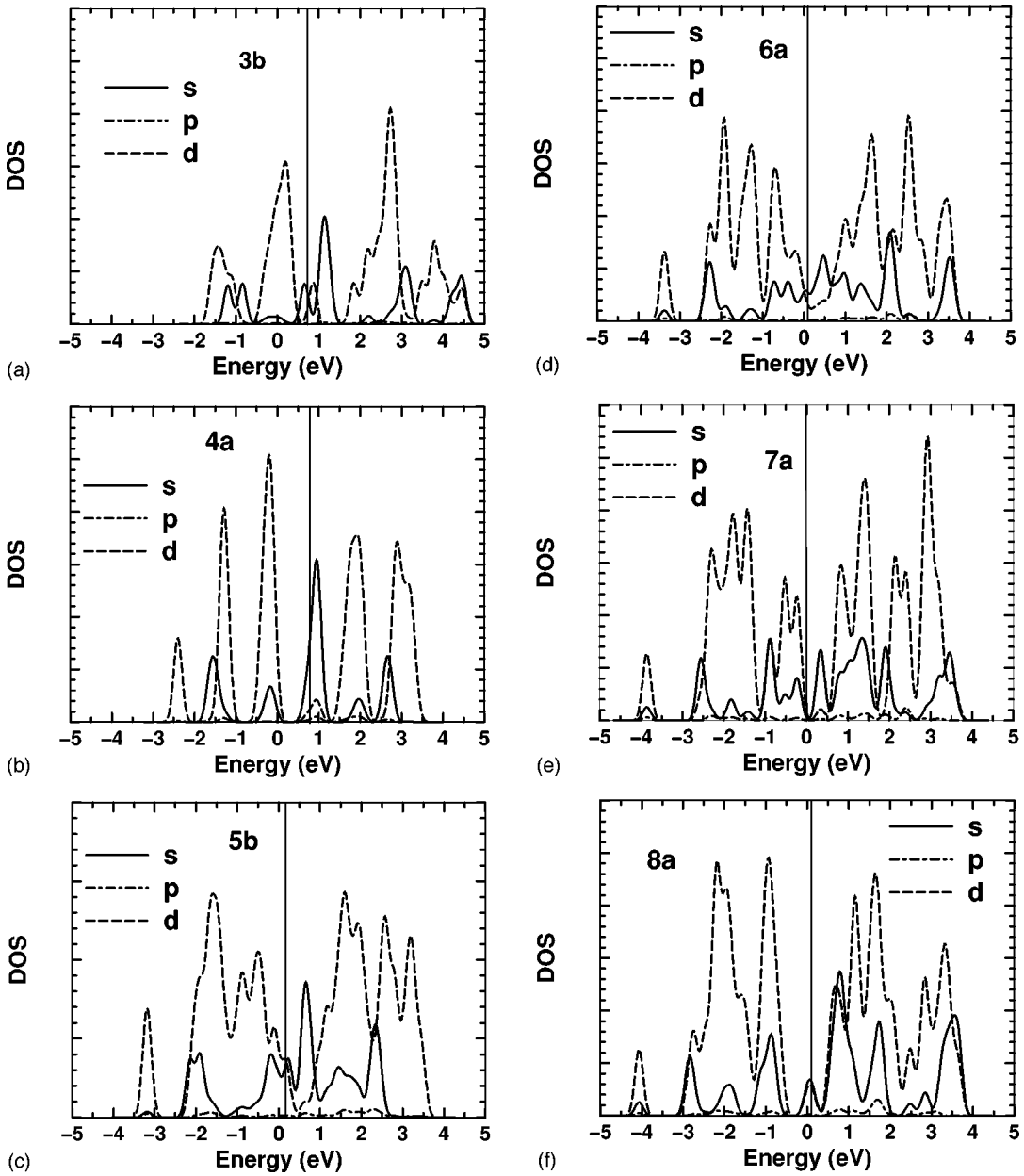

FIG. 5. Electronic density of states (DOS) of niobium cluster anions (a) $3b$, (b) $4a$, (c) $5b$, (d) $6a$, (e) $7a$, and (f) $8a$. The vertical line is drawn at the Fermi energy $[(\epsilon^{\mathrm{HOMO}}+\epsilon^{\mathrm{LUMO}})/2]$.

cluster size in a way that is typical for clusters. By Nb_8^- the calculated B is still only about 74% of the experimental bulk cohesive energy (7.57 eV/atom) and it is very likely that our LSD calculations overestimate all binding energies. The value of B for Nb_8^- that we get from data in Refs. [40] and [13] is 5.1 eV/atom, or 67% of the cohesive energy. We compared the electron affinities (A) to those that we calculate for a conducting spherical droplet (CSD) model [2] by taking 4.3 eV as the work function of niobium, and cluster radii consistent with our DFT optimized geometries. The CSD model overestimates electron affinities by amounts going roughly from 0.3 to 1.0 eV (0.5 eV on average). Details of the electronic structure, which are ignored in the CSD model, are responsible for variations of roughly 0.7 eV in the electron affinities. Similar variations are found among the electron affinities of different cluster isomers (see Table III). There is a range of bond lengths among the different clusters and even *within* some of the clusters (e.g., $6a$). Typical bond lengths are between 2.4 and 2.9 Å, the latter corresponding to the bulk interatomic distance (2.86 Å). If we define bonded atom pairs as those having interatomic distances less than 3 Å, the average bond length in clusters $3a$ through $8a$ respectively is 2.31, 2.48, 2.53, 2.57, 2.59, and 2.58 Å. We expect an accuracy of about 0.05 Å or better in our LSD calculations, so the bond lengths in Nb_8^- are still very far from those of the bulk. Yet, it is not impossible that the average bond length increases sharply and gets near 2.86 Å for cluster sizes between 10 and 20. That could happen if the presence of one or more interior atoms with a high coordination and distances to its neighbors close to 2.86 Å places constraints on the overall structure of the cluster.

TABLE III. Binding energy (in eV) per atom (B), and energy for dissociation (E), disproportionation (D), and ionization (A) of niobium cluster anions (see text).

	B	E	D	A
2a	2.83	5.65	+0.05	1.10
3a	3.73	5.57	−1.24	1.14
3b	3.70			1.06
3c	2.80			1.66
4a	4.51	6.82	+0.50	0.89
4b	4.31			0.79
4c	3.30			1.83
5a	4.87	6.32	+0.08	1.62
5b	4.81			1.66
5c	4.46			1.86
5d	4.44			1.88
6a	5.10	6.24	−0.98	1.63
6b	4.98			1.41
6c	4.28			2.05
7a	5.40	7.22	+0.49	1.90
7b	5.27			1.92
7c	5.19			1.45
7d	5.18			1.73
7e	5.17			1.70
7f	5.15			1.72
8a	5.57	6.73		1.55
8b	5.44			1.63
8c	5.42			1.71
8d	5.36			1.91

IV. SUMMARY AND CONCLUSION

The Slater's transition state can be a very helpful tool for elucidating cluster structure. It is easy to implement, its efficiency allows calculating the hundreds of BEs typically needed for comparing to experiment, and the accuracy for niobium cluster anions was sufficient to assign the structure. For other elements or larger clusters, calculation of BEs alone may not be sufficient to assign structure with confidence: calculating the photoionization cross section may be necessary. Practical approximate methods for cross-section calculations [43] must be developed or else the computing requirement for moderate size clusters will be prohibitive. The STS method should also prove useful in calculations of photoabsorption spectra of metal clusters. We did preliminary tests for transition metal clusters in the range from three to seven atoms and found that STS calculations are very fast. The calculation of all the valence excitation energies and oscillator strengths needed for modeling a UV-visible spectrum (as many as 780 in Nb_7) requires a computing effort that is of the same order as that for a geometry optimization. It remains to be seen whether such calculations are accurate enough to give reliable assignments of experimental spectra.

The four-atom and seven-atom clusters of niobium appear to be particularly stable irrespective of the electric charge $(-1,\ 0,\ +1)$ on the cluster. This is inconsistent with the simplest jellium models where electronic shell closings that occur for particular number of electrons are responsible for the extra stability of some clusters. But it is consistent with the assumption that geometric structure is the key factor determining stability, and our observation that the geometries of neutral and anion clusters are very similar. We believe that the structural similarity between neutrals and anions is essentially due to niobium being near the middle of the transition metal series: since the binding energy is large and involves many localized d bonding orbitals in addition to the usual delocalized s bonding, addition or removal of essentially nonbonding electrons at E_F has a small effect. But even for open d-shell metals like niobium the jellium model is useful for interpreting the results of a more accurate theory. The trend in our calculated electron affinities agrees roughly with the CSD model, the magnitude of the discrepancies gives insight into how much cluster isomerism can affect a physical property.

ACKNOWLEDGMENTS

Work at the University of Nevada, Las Vegas was supported in part by NSF Grant No. OSR-9353227, the DOE EPSCoR program, and the W. M. Keck Foundation. Figures were prepared with XMol version 1.3.1 (Minnesota Supercomputer Center, Inc., Minneapolis, MN) and XMgr v3.01pl7 (Paul J. Turner).

[1] W. A. de Heer, Rev. Mod. Phys. **65**, 611 (1993); M. Brack, *ibid.* **65**, 677 (1993).

[2] J. P. Perdew, Phys. Rev. B **37**, 6175 (1988); G. Makov, A. Nitzan, and L. E. Brus, J. Chem. Phys. **88**, 5076 (1988).

[3] C. Ellert *et al.*, Phys. Rev. Lett. **75**, 1731 (1995).

[4] B. K. Rao, P. Jena, and A. K. Ray, Phys. Rev. Lett. **76**, 2878 (1996); H. W. Sarkas, S. T. Arnold, J. H. Hendricks, and K. H. Bowen, J. Chem. Phys. **102**, 2653 (1995).

[5] B. I. Dunlap, Phys. Rev. A **41**, 5691 (1990).

[6] M. B. Knickelbein and S. Yang, J. Chem. Phys. **93**, 1476 (1990); E. K. Parks, B. J. Winter, T. D. Klots, and S. J. Riley, *ibid.* **94**, 1882 (1991); L. Lian, C.-X. Su, and P. B. Armentrout, *ibid.* **97**, 4072 (1992); **97**, 4084 (1992); E. K. Parks, T. D. Klots, B. J. Winter, and S. J. Riley, *ibid.* **99**, 5831 (1993); G. M. Koretsky and M. B. Knickelbein, *ibid.* **106**, 9810 (1997).

[7] E. L. Muetterties *et al.*, Chem. Rev. **79**, 91 (1979); M. D. Morse, M. E. Geusic, J. R. Heath, and R. E. Smalley, J. Chem. Phys. **83**, 2293 (1985); M. Moskovits, J. Mol. Catal. **82**, 195 (1993).

[8] Examples of this are C_{60} [H. W. Kroto *et al.*, Nature (London) **318**, 162 (1985)]; Ti_8C_{12} [B. C. Guo, K. P. Kerns, and A. W. Castleman, Jr., Science **255**, 1411 (1992)]; and Si_{45} [U. Röthlisberger, W. Andreoni, and M. Parrinello, Phys. Rev. Lett. **72**, 665 (1994)].

[9] R. J. Van Zee and W. Weltner, Jr., J. Chem. Phys. **92**, 6976 (1990); S. Riley, in *Clusters of Atoms and Molecules; Theory, Experiments, and Clusters of Atoms*, edited by H. Haberland (Springer, Berlin, 1994), p. 221; R. O. Jones, G. Ganteför, S.

Hunsicker, and P. Pieperhoff, J. Chem. Phys. **103**, 9549 (1995).
[10] J. Blanc *et al.*, J. Chem. Phys. **96**, 1793 (1992).
[11] V. Bonačić-Koutecký *et al.*, J. Chem. Phys. **100**, 490 (1994).
[12] D. S. Yang *et al.*, J. Chem. Phys. **103**, 5335 (1995).
[13] H. Kietzmann *et al.*, Phys. Rev. Lett. **77**, 4528 (1996).
[14] G. Ganteför, M. Gausa, K.-H. Meiwes-Broer, and H. O. Lutz, J. Chem. Soc., Faraday Trans. **86**, 2483 (1990); H. Yoshida *et al.*, J. Chem. Phys. **102**, 5960 (1995); L.-S. Wang, H.-S. Cheng, and J. Fan, *ibid.* **102**, 9480 (1995); M. Iseda *et al.*, *ibid.* **106**, 2182 (1997).
[15] D. S. Yang, A. M. James, D. M. Rayner, and P. A. Hackett, J. Chem. Phys. **102**, 3129 (1995); D.-S. Yang *et al.*, Chem. Phys. Lett. **227**, 71 (1997).
[16] M. B. Knickelbein and W. J. C. Menezes, Phys. Rev. Lett. **69**, 1046 (1993); W. C. J. Menezes and M. B. Knickelbein, J. Chem. Phys. **98**, 1867 (1993); B. A. Collings, K. Athanassenas, D. M. Rayner, and P. A. Hackett, Z. Phys. D **26**, 36 (1993); Chem. Phys. Lett. **227**, 490 (1994); B. A. Collings *et al.*, J. Chem. Phys. **101**, 3506 (1994).
[17] M. R. Zakin *et al.*, J. Chem. Phys. **85**, 1198 (1986); D. M. Rayner *et al.*, in *Theory of Atomic and Molecular Clusters*, edited by J. Jellinek (Springer, Berlin, 1998).
[18] J. C. Slater, Phys. Rev. **81**, 385 (1951); J. C. Slater, Adv. Quantum Chem. **6**, 1 (1972).
[19] A. R. Williams, R. A. deGroot, and C. B. Sommers, J. Chem. Phys. **63**, 628 (1975); D. P. Chong, Chem. Phys. Lett. **232**, 486 (1995).
[20] A. St-Amant and D. R. Salahub, Chem. Phys. Lett. **169**, 387 (1990); A. St-Amant, Thèse de doctorat, Université de Montréal, 1992.
[21] S. H. Vosko, L. Wilk, and M. Nusair, Can. J. Phys. **58**, 1200 (1980).
[22] J. Andzelm, E. Radzio, and D. R. Salahub, J. Chem. Phys. **83**, 4573 (1985).
[23] L. Goodwin and D. R. Salahub, Phys. Rev. A **47**, R774 (1993).
[24] A. M. James, P. Kowalczyk, R. Fournier, and B. Simard, J. Chem. Phys. **99**, 8504 (1993).
[25] The molecular orbitals are expanded in a Cartesian Gaussian basis set having the pattern (41111/4111/411), where the number of primitives in each contraction is listed, first for s-type functions, then p-type and d-type. Two auxiliary sets of Cartesian Gaussians are used to fit the electron density and the exchange-correlation potential, each consisting of four s-type functions and five shells of s-, p-, and d-type Cartesians sharing the same exponents, for a total of 54 fitting functions in each auxiliary set. The potential due to the atom's $1s^2 2s^2 2p^6 3s^2 3p^6 3d^{10} 4s^2$ frozen core is described by five spherical Gaussians, and orthogonality of the valence orbitals to the core is enforced by projectors written in a basis of eight s, five p, and four d Cartesian Gaussians. Exponents and coefficients for these basis sets are available upon request to the authors.
[26] R. Fournier, J. Andzelm, and D. R. Salahub, J. Chem. Phys. **90**, 6371 (1989); I. Pápai, A. St-Amant, J. Ushio, and D. R. Salahub, Int. J. Quantum Chem. **S24**, 29 (1990).
[27] A. D. Becke, Phys. Rev. A **38**, 3098 (1988).
[28] J. P. Perdew, Phys. Rev. B **33**, 8822 (1986); J. P. Perdew and Y. Wang, *ibid.* **33**, 8800 (1986).
[29] A. Garciá, C. Elässer, J. Zhu, S. G. Louie, and M. L. Cohen, Phys. Rev. B **46**, 9829 (1992).
[30] A more rigorous treatment of excited states in DFT is possible, but at the present time it is impractical for large systems such as our Nb clusters. See, e.g., M. Casida, in *Recent Advances in Density Functional Methods*, Vol. 1, edited by D. P. Chong (World Scientific, 1995, Singapore), and references therein.
[31] T. Ziegler, A. Rauk, and E. J. Baerends, Theor. Chim. Acta **43**, 261 (1977).
[32] C. Massobrio, A. Pasquarello, and R. Car, Phys. Rev. Lett. **75**, 2104 (1995).
[33] P. Duffy and D. P. Chong, Organic Mass Spectrom. **28**, 321 (1993); D. P. Chong, J. Chem. Phys. **103**, 1842 (1995).
[34] J. Koutecký and P. Fantucci, Chem. Rev. **86**, 539 (1986); V. Bonačić-Koutecký, P. Fantucci, and J. Koutecký, J. Chem. Phys. **93**, 3802 (1990); V. Bonačić-Koutecký, P. Fantucci, and J. Koutecký, *ibid.* **98**, 7981 (1993).
[35] M. S. Stave and A. E. DePristo, J. Chem. Phys. **97**, 3386 (1992).
[36] J.-Y. Yi, D. J. Oh, and J. Bernholc, Phys. Rev. Lett. **67**, 1594 (1991); M. Castro and D. R. Salahub, Phys. Rev. B **49**, 11 842 (1994); C. Jamorski, A. Martinez, M. Castro, and D. R. Salahub, *ibid.* **55**, 10 905 (1997).
[37] J. F. Janak, Phys. Rev. B **18**, 7165 (1978).
[38] H. B. Shore, J. H. Rose, and E. Zaremba, Phys. Rev. B **15**, 2858 (1976).
[39] A more detailed discussion of anion's stability in DFT methods can be found in N. Rösch and S. B. Trickey, J. Chem. Phys. **106**, 8940 (1997); see also J. M. Galbraith and H. F. Schaefer III, *ibid.* **105**, 862 (1996).
[40] D. A. Hales, L. Lian, and P. B. Armentrout, Int. J. Mass Spectrom. Ion Phys. **102**, 269 (1990).
[41] M. B. Knickelbein and S. Yang, J. Chem. Phys. **93**, 5760 (1990).
[42] M. B. Knickelbein, Chem. Phys. Lett. **192**, 129 (1992).
[43] A. Görling and N. Rösch, J. Chem. Phys. **93**, 5563 (1990).